Applied Radiation and Isotopes 69 (2011) 1826–1829

Contents lists available at ScienceDirect

Applied Radiation and Isotopes

journal homepage: www.elsevier.com/locate/apradiso

Computational dosimetry of a simulated combined standard X-Rays and BNCT treatment

M.R. Casal [a,b,*], M.S. Herrera [b,c,d], S.J. González [b,c], D.M. Minsky [b,c,d]

[a] Instituto de Oncología "Ángel H. Roffo", Universidad de Buenos Aires, Av. San Martín 5481, Bs.As., Argentina
[b] Comisión Nacional de Energía Atómica, Av. General Paz 1499, San Martín, Buenos Aires, Argentina
[c] Consejo Nacional de Investigaciones Científicas y Técnicas (CONICET) Av. Rivadavia 191, Buenos Aires, Argentina
[d] Escuela de Ciencia y Tecnología, Universidad de General San Martín, 25 de Mayo and M. de Irigoyen, San Martín, Argentina

ARTICLE INFO

Available online 17 February 2011

Keywords:
BNCT
LINAC
MCNP
NCTPlan
DVHTool

ABSTRACT

There has been increasing interest in combining Boron Neutron Capture Therapy (BNCT) with standard radiotherapy, either concomitantly or as a BNCT treatment of a recurrent tumor that was previously irradiated with a medical electron linear accelerator (LINAC). In this work we report the simulated dosimetry of treatments combining X-rays and BNCT

1. Introduction

Radiotherapy is one of the standard treatments for many malignancies. According to the United States National Cancer Institute 50% of cancer patients are treated with radiation therapy in some stage of their treatment, either alone, or in combination with other types of cancer treatment.

It is also known that some of these malignancies will recur, and, if standard radiation therapy is intended to be used again, the dose to the tumor may be limited by the dose already delivered to normal tissues. BNCT appears to be a good alternative to treat this kind of cases, as the differential boron uptake in tumor cells makes it possible to prescribe high doses to the tumor, while keeping the doses in normal tissues well below tolerance values (Kato et al., 2009; Kimura et al., 2009; Kankaanranta et al., 2007). Some authors have also shown that combined BNCT and standard fractionated radiation therapy could lead to a therapeutic gain in some highly malignant tumors (Barth et al., 2004; Matusumura et al., 2009). There are new ongoing clinical trials combining BNCT with standard fractionated radiotherapy and chemotherapy (Yamamoto et al., 2010, Kawabata et al., 2010) to treat newly diagnosed malignant glioblastoma

In order to calculate the combined dosimetry of a patient, who has to undergo different radiation regimes, and evaluate normal tissue complication probabilities, dose–volume histograms (DVHs) that combine the results of the different phases of the treatment are useful.

This work describes the generation of an accelerator model that can be included in the tools currently used to evaluate treatment planning in the Argentine BNCT protocols. The results of a simulated combined standard fractionated radiation therapy and BNCT treatment for a clinical case are also shown.

2. Materials and methods

2.1. Monte Carlo Modeling of a LINAC and generation of the X-ray source

In a first step, a model of a Siemens Primus Linear Accelerator was developed and adjusted with experimental data. This LINAC is installed at the Radiation Therapy Department of Instituto de Oncología "Ángel H. Roffo".

The detailed geometry and composition of all components in the beamline were provided by the manufacturer – Siemens Healthcare, USA – and was modeled in the MCNP5 (LANL, 2003) code. According to the work by several authors (Mohan and Chui, 1985; Sheik-Bagheri and Rogers, 2002), the parameters of the electron beam impinging on the target were adjusted with experimental data available at the hospital, namely depth–dose curves and lateral dose profiles measured in a Scanditronix–Wellhoffer water phantom with a 0.3 cc PTW ionization chamber. The energy and spatial distribution of the electron beam were assumed to be Gaussian. The initial parameters for the 6 MV X-Ray beam, namely, full width at half maximum (FWHM) and mean of the electron energy distribution,

* Corresponding author at: Instituto de Oncología "Ángel H. Roffo", Universidad de Buenos Aires, Av. San Martín 5481, Bs.As., Argentina.Tel.: +5411 4501 8374; fax: +5411 4580 2811.
E-mail addresses: mcasal@cnea.gov.ar (M.R. Casal), mariettaherrera@gmail.com (M.S. Herrera), srgonzal@cnea.gov.ar (S.J. González), minsky@tandar.cnea.gov.ar (D.M. Minsky).

0969-8043/$ - see front matter © 2011 Elsevier Ltd. All rights reserved.
doi:10.1016/j.apradiso.2011.02.023

and its spatial FWHM were also provided by the manufacturer. These parameters were then corrected to match experimental data: the mean energy of the beam was adjusted according measured depth–dose curves and the spatial width was adjusted to match the lateral dose profiles at 10 cm depth, beyond the range of the contaminant secondary electrons produced in the collimator jaws. Adjustments in the FWHM and mean value of the electron energy distribution were made iteratively until the differences between measured and calculated values were within the tolerances recommended by international protocols (IAEA, 2004). The MCNP simulation was performed, 5×10^7 source electron histories were run, and the ITS electron transport algorithm was used. In order to minimize calculation times, a photon cut-off energy of 10 keV was chosen for all cells. The electron cut-off energy was selected cell by cell: 100 keV in critical cells such as target and water phantom and 1.5 MeV in collimators.

The resulting accelerator model was used to generate a planar track-by-track surface source in a plane located between the accelerator monitor chambers and the secondary collimators that define the beam size (see Fig. 1); in this way, the patient dependent elements such as secondary collimators, blocks, or wedges can be adjusted to provide the desired configuration, without performing the transport in the whole geometry. No variance reduction methods were used to generate the surface source, and both photon and electron cut-off energies were 10 keV. Calculations in a water phantom were performed once more with this source, and compared with experimental data. The LINAC calibration factor in reference conditions was used to calculate a normalization factor for the photon source, in terms of the LINAC's monitor units.

The generated surface source, fully compatible with NCTPlan (González et al., 2002a; González et al., 2005) treatment planning system (TPS) was ultimately used to perform the calculations in the patient geometry.

2.2. Neutron source

An accelerator-based BNCT (AB-BNCT) source, currently under development at the CNEA, was chosen to provide the neutron beam. Based on the ^{7}Li(p,n)^{7}Be reaction at 2.6 MeV and 30 mA (Lee and Zhou, 1999) theoretical neutron yield for this reaction was considered for a lithium fluoride target. An optimized beam shaping assembly (Minsky et al., 2010) was employed to obtain an epithermal neutron beam centered at approximately 10 keV.

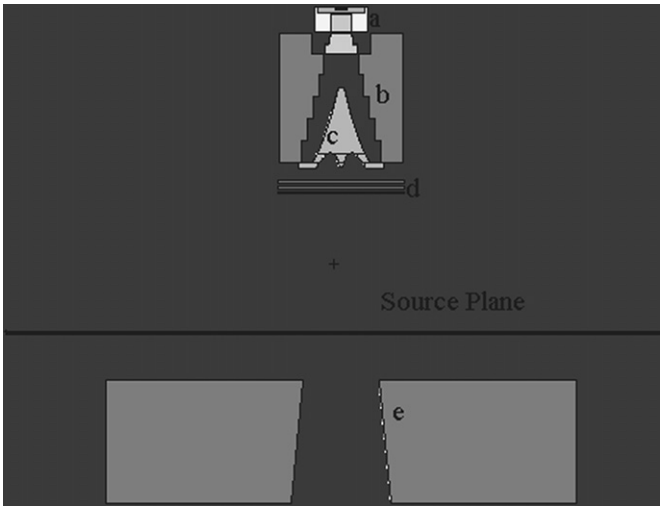

Fig. 1. Main LINAC components in the accelerator beamline: target (a), primary collimator (b), flattening filter (c), monitor chambers (d), and secondary collimators (e).

2.3. Patient geometry, treatment planning, and dose evaluation

As an example to test the implementation of the accelerator X-Ray source and the combination of a standard X-Ray treatment and a BNCT treatment, a CT study of a patient with a central nervous system tumor was used. The CT stack was voxelized using NCTPlan, following the same procedure used for treatment planning in the Argentine metastatic cutaneous melanoma clinical trial. This voxel model was used to perform the calculations for both the X-Ray and the mixed neutron–gamma BNCT beam. NCTPlan was also used to position the radiation beams and prepare the input file for the MCNP code for both treatments. The variable secondary collimator was considered part of the modeled geometry. In this way, only one planar source is needed, and the aperture of the collimator jaws can be adjusted to fit each individual case. Although the secondary collimator geometry is fairly simple, the selected strategy was to fix the planar source and the secondary collimator, and rotate the patient geometry around them.

Once the output files for each beam have been calculated, they were used as input in NCTPlan to display the isodose curves. The DVHs were calculated with DVHTool system (González et al., 2002b) for two regions of interest, brain and tumor.

3. Results and discussion

3.1. LINAC model

The dose was calculated tallying the photon flux (F4:P in MCNP), multiplied by the absorption coefficients in water, as is the standard procedure in BNCT gamma dose calculations.

To establish the agreement between the calculated and the measured data for the LINAC model, depth–dose curves and lateral beam profiles for beam sizes of 5×5, 10×10, 20×20, and 40×40 cm^2, were used.

The first evaluated magnitude was the beam quality index, D_{10}^{20} as defined in IAEA TRS 398 (IAEA, 2000). This is calculated as the quotient of the dose at 20 and 10 cm depths, and is used in standard radiotherapy beams as an indicator of the photon spectrum. The calculated $D_{10,calc}^{20}$ is 0.575 and the measured $D_{10,meas}^{20}$ 0.580.

The indicator suggested in international protocols (IAEA, 2004) to quantify deviations between the results of calculations and measurements in depth–dose curves and lateral profiles is the percent relative difference, δ.

According to the work of Venselaar et al. (2001) and international protocols, δ values are calculated separating depth–dose curves and lateral beam profiles in different regions: δ_1 measures the relative difference in depth–dose curves in the central beam axis for the high dose–low gradient region; δ_2 measures relative differences in high dose–high gradient regions (build-up region in depth–dose curves and penumbra in lateral profiles); δ_3 takes into account relative differences in high dose–low gradient regions in lateral profiles; δ_4 measures the dose differences in points outside the radiation beam.

Table 1 shows the results of the evaluation and the corresponding tolerance values for the above mentioned regions As can be observed in the table, all evaluated quantities are within the recommendations of IAEA TRS-430,except for the build-up region. Although the product of photon flux and the absorption coefficient in water is considered a reasonable and conservative quantity to represent the dose in BNCT, it highly overestimates the actual dose in the build-up region for the case of megavoltage X-rays. In order to improve the dose estimation in the build-up region, a second try was to calculate the average electron flux modified by the energy-dependent response function given by the collision stopping power taken from NIST. This strategy provides a

much better agreement in the build-up zone, with $\delta_2 = 4.4\%$ (2 mm), and was chosen instead of an energy deposition tally such as *F8, because results with both methods are coincident within statistical errors, and the track length estimator F4 allows the use of the FMESH tool, making calculations much faster. It should be noted that results computed in this manner have a higher statistical error than those obtained with the photon flux for the same number of source particles (3.5% vs. 0.7%).

3.2. Treatment planning and dose evaluation

The selected beam arrangement consisted in one BNCT posterior field (beam aperture 25×25 cm^2) and two lateral opposed, 5×5 cm^2, 6 MV photon fields. Although this is not a beam configuration normally chosen in a 3D X-ray conformal treatment, the isodose curves for this simple arrangement are well known and thus allow visualizing the contribution of each type of treatment to the total isodoses, and make noticeable any problem in the beam location. The X-ray dose was 50 Gy in 25 fractions; the BNCT dose was chosen so the maximum dose in normal brain due to both treatments was 16 Gy-Eq. Single fraction equivalent dose for the X-treatment was calculated using the standard linear quadratic model.

Fig. 2(a) and (b) shows the dose distribution in normal tissue for a simulated X-ray–BNCT combined treatment, calculated using photon and electron flux, respectively. The displayed isodose curves are normalized to the normal tissue maximum dose and were calculated using the kerma factors for skin. It can be observed that the main contribution for the dose in normal brain is due to the X-Ray fields, and the difference in the skin dose is noticeable, depending on the tally used to evaluate the dose.

In Fig. 3 the DVHs for the simulated treatment are shown. They were calculated with DVHTool, using the MCNP output and a Region Of Interest (ROI) file generated with NCTPlan. The dose files were calculated with the F4:E tally (Fig. 3(a) and (b)).

Table 1
Relative differences "δ" between measured and calculated doses in different regions of interest as defined by Venselaar (2001) and recommended by international protocols (IAEA, 2004); δ_1 defined in high dose–low gradient region in PDD curve, δ_2 in high dose–high gradient region, δ_3 calculated in high dose–low gradient region in lateral profiles, and δ_4 outside the radiation field.

Region	δ based on F4:P	δ Recommended (TRS-430)
δ_1	1%	2%
δ_2 (build-up)	21% 5 mm	10% or 2 mm
δ_2 (penumbra)	10% 1 mm	
δ_3	2%	3%
δ_4	25%	30%

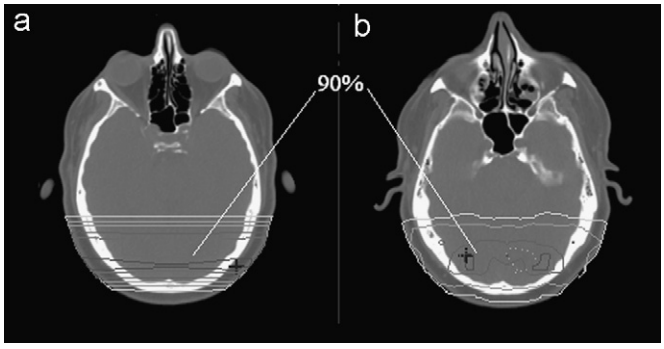

Fig. 2. Isodose curves for normal tissue, calculated using (a) photon flux and (b) electron flux. The CT slice in each case corresponds to the location of the global maximum for normal tissue (cross), chosen as normalization value. 90% isodose reaches the skin in case (a), while it closes deeper in tissue in case (b).

4. Conclusions

The LINAC model provided an easily handled planar surface source that could be used in treatment planning systems currently employed in the Argentine clinical trials to generate the MCNP input and perform the treatment planning calculations. The resulting dose matrix was compatible with NCTPlan, without needing any modification, and the dose distributions could be displayed and DVHs calculated in DVHTool. The generated LINAC model is then ready to be used to perform calculations for a combined treatment.

When using average photon flux to calculate the dose due to the LINAC source, the overestimation of the dose in the build-up region leads to a false maximum dose on the skin in the simulated clinical case. This may be an important aspect of dose evaluation, especially in cases where skin is considered an organ at risk, and thus it can limit the dose administered to the target. This miscalculation can be avoided using the electron flux to estimate the dose; however, in order to obtain similar statistical errors, the number of histories (and consequently, the computation time) needs to be increased, compared with the time needed when calculating photon flux. For this case, variance reduction techniques should be used to minimize the computation time and to attain acceptable statistical errors. The use of such techniques in our calculations is being implemented.

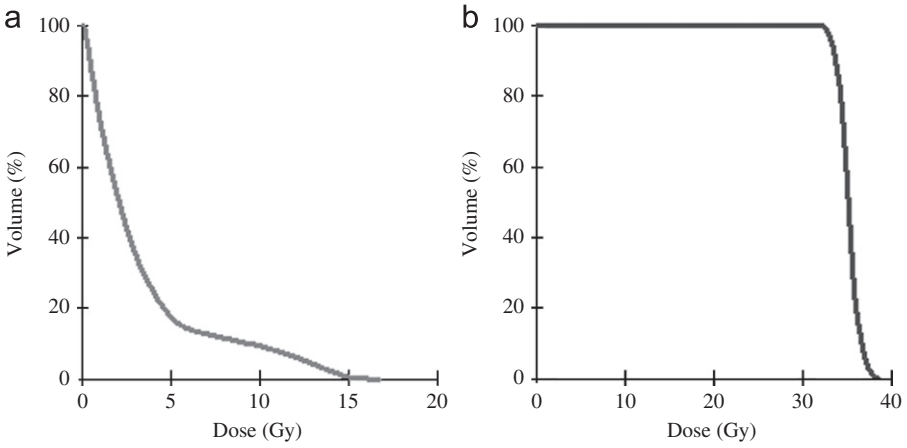

Fig.3. DVHs generated by DVHTool for: (a) normal brain and (b) tumor. Dose calculated with F4:E tally.

References

Barth, R.F., Grecula, J.C., Yang, W., Rotaru, J., Nawrocky, M., Gupta, N., Albertson, B.J., Ferketich, A.K., Moeschberger, M.L., Coderre, J.A., Rofstad, E.K., 2004. Combination of Boron Neutron Capture Therapy and External Beam Radiotherapy for brain tumors. Int. J. Radiat Oncol. Biol. Phys. 59 (1), 267–277.

González, S.J., Santa Cruz, G.A., Kiger III, W.S., Goorley, T., Palmer, M.R., Busse, P.M., Zamenhof, R.G., 2002a. NCTPlan, the New PC version of MacNCTPlan: improvements and verification of a BNCT treatment planning system. In: Sauerwein, W., Moss, R., Wittig, A., (Eds.). Proceedings of the 10th International Congress on Neutron Capture Therapy. Monduzzi Editore, Bologna, pp. 557–561.

González, S.J., Carando, D.G.., Santa Cruz, G..A., Zamenhof, R.G., 2005. Voxel model in BNCT treatment planning: performance analysis and improvements. Phys. Med. Biol. 50, 441–458.

González, S.J., Santa Cruz, G.A., Kiger III, W.S., Zamenhof, R.G., 2002b. A new computational tool for constructing dose–volume histograms using combinatorial techniques. In: Sauerwein, W., Moss, R., Wittig, A. (Eds). Proceedings of the Tenth International Congress on Neutron Capture Therapy. Monduzzi Editore, Bologna, pp. 629–633.

IAEA, 2000. Absorbed dose determination in external beam radiotherapy: an international code of practice for dosimetry based on standards of absorbed dose to water. Technical report series 398. IAEA, Viena.

IAEA, 2004. Commissioning and quality assurance of computerized planning systems for radiation treatment of cancer. Technical report series 430. IAEA, Viena.

Lee, C.L., Zhou, X.L., 1999. Thick target neutron yields for the 7Li(p,n)7Be reaction near threshold. Nucl. Instrum. Methods B 152, 1–11.

Kankaanranta, L., Seppala, T., Koivunoro, H., Saarilahti, K., Atula, T., Collan, J., Salli, E., Kortesniemi, M., Uusi-Simola, J., Mäkitie, A., Peppänen, M., Minn, H., Kotiluoto, P., Auterinen, I., Savolainen, S., Kouri, M., Joensuu, H., 2007. Boron Neutron Caputrue Therapy in the treatment of locally recurred head and neck cancer. Int. J. Radiat. Oncol. Biol. Phys. 69 (2), 475–482.

Kato, I., Fujita, Y., Maruhashi, A., Maruhashi, A., Kumada, H., Ohmae, M., Kirihata, M., Imahori, Y., Suzuki, M., Sakrai, Y., Sumi, T., Iwai, S., Nakazawa, M., Murata, I., Miyamaru, H., Ono, K., 2009. Effectiveness of boron neutron capture therapy for recurrent head and neck malingnancies. Appl. Radiat. Isot. 67, S37–S42.

Kawabata, S., Miyatake, S-I., Hiramatsu, R., Miyata, S., Takekita, Y., Doi, A., Kuroiwa, T., Kirihata, M., Sakurai, Y., Maruhashi, A., Ono, K., 2010. Phase II clinical study of Boron Neutron Capture Therapy combined with X-ray radiotherapy/temozolomide in patients with newly diagnosed glioblastoma multiforme—current status report. In: Liberman, Kreiner, Casal, et al. (Eds.). New Challenges in Neutron Capture Therapy. Proceedings of 14th International Congress on Neutron Capture Therapy. CNEA, Buenos Aires, pp. 9–12.

Kimura, Y., Ariyosi, Y., Shimahara, M., Miyatake, S., Kawabata, S., Ono, K., 2009. Boron Neutron Capture Therapy for recurrent oral cancer and metastasis of cervical lymph node. Appl. Radiat. Isot. 67, S47–S49.

LANL, 2003. A General Monte Carlo N Particle Transport Code, version 5, LA-UR-03-1987, Los Alamos National Laboratory.

Matusumura, A., Yamamoto, T., Tsurubuchi, T., et al., 2009. Current practices and future directions of therapeutic strategy in glioblastoma: Survival benefit and indication of BNCT. Appl. Radiat. Isot. 67, S12–S14.

Minsky D.M., Kreiner A.J., Valda A.J., 2010. AB-BNCT beam shaping assembly based on 7Li(p,n)7Be reaction optimization. In: Liberman, Kreiner, Casal, et al. (Eds.), New Challenges in Neutron Capture Therapy. Proceedings of 14th International Congress on Neutron Capture Therapy. CNEA, Buenos Aires,. pp 476–479.

Mohan, R., Chui, C., 1985. Energy and angular distributions of photons from medical linear accelerators. Med. Phys. 12 (5), 592–597.

Sheik-Bagheri, D., Rogers, D.W.O., 2002. Sensitivity of megavoltage photon beam Monte Carlo simulations to electron beam and other parameters. Med. Phys. 29 (3), 379–390.

Venselaar, J., Wellenveerd, H., Mijnheer, B., 2001. Tolerances for the accuracy of photon beam dose calculations of treatment planning systems. Radiother. Oncol. 60, 191–201.

Yamamoto, T., Nakai, K., Nariai, T., Kumada, H., Okumura, T., Mizumoto, M., Tsuboi, K., Zaboronok, A., Ishikawa, E., Aiyama, H., Endo, K., Takada, T., Yoshida, F., Shibata, Y., Matsumura, A., 2010. The status of Tsukuba BNCT Trial: BPA-based Boron Neutron Capture Therapy combined with X-ray irradiation. In: Liberman, Kreiner, Casal, et al.(Eds.), New Challenges in Neutron Capture Therapy. Proceedings of 14th International Congress on Neutron Capture Therapy. CNEA, Buenos Aires, pp. 7–8.